Iberian Margin sea surface temperature during MIS 15 to 9 (580–300 ka): Glacial suborbital variability versus interglacial stability

T. Rodrigues,[1,2] A. H. L. Voelker,[1,2] J. O. Grimalt,[3] F. Abrantes,[1] and F. Naughton[1,2]

Received 8 January 2010; revised 16 September 2010; accepted 22 November 2010; published 15 February 2011.

[1] Past sea surface water conditions of the western Iberian Margin were reconstructed based on biomarker analyses of a marine deep sea core MD03-2699 from the Estremadura Spur north off Lisbon, providing new insights into orbital and suborbital-scale climate variability between marine isotope stage (MIS) 15 to MIS 9 (580 to 300 ka). We use biomarker-based proxy records such as the alkenone unsaturated index to estimate sea surface temperature (SST), the total alkenone concentration to reconstruct phytoplankton productivity, and terrestrial biomarkers to evaluate the continental input. The results extend the existing biomarker record, namely the SST for the Iberian Margin, back to the sixth climatic cycle (580 ka). A general trend of stable interglacials contrasts with glacial periods and glacial inceptions which are marked by high-frequency variability. Thus, several short-lived climatic coolings were identified by large SST decreases, the occurrence of ice-rafted detritus and high percentages of the tetraunsaturated alkenone $C_{37:4}$. Some of these events were extremely cold and similar in their general trends to the well-known Heinrich events of the last glaciation. We identified eight Heinrich-type events between 580 and 300 ka. The general deglaciation pattern detected between MIS 15 and MIS 9 is similar in their general trends to that characterizing the more recent climatic cycles, i.e., marked by two coolings separated by a short warming episode which may reflect the southward, northward, and southward migration of the Polar Front.

Citation: Rodrigues, T., A. H. L. Voelker, J. O. Grimalt, F. Abrantes, and F. Naughton (2011), Iberian Margin sea surface temperature during MIS 15 to 9 (580–300 ka): Glacial suborbital variability versus interglacial stability, *Paleoceanography*, *26*, PA1204, doi:10.1029/2010PA001927.

1. Introduction

[2] The Earth's climate gradually cooled during the past 5 Ma [*Lisiecki and Raymo*, 2005; *Zachos et al.*, 2001; *Shackleton*, 1967; *Maslin et al.*, 1998]. Within this long-term climate trend several orbital-induced climate oscillations, with periodicities of 21 kyr, 41 kyr and 100 kyr have been observed in numerous deep sea cores distributed throughout the global ocean [*Lisiecki and Raymo*, 2005]. A transition from prevailing symmetrical low-amplitude and high-frequency ice volume variations (41 kyr) to prevailing asymmetrical high-amplitude and low-frequency ice volume variations (100 kyr) is attributed to the climate transition called the Mid-Pleistocene Revolution (MPR) [*Imbrie et al.*, 1993]. This change was in agreement with a variation in the mean state of the global climate system, involving an evolution toward lower atmospheric temperatures and higher global ice volume [*Shackleton et al.*, 1990]. After this event (around 430 ka) the global climate became mainly controlled by the 100 kyr cyclicity [*Loutre and Berger*, 2003] and started to be characterized by relatively short warm episodes during interglacials and longer cold phases during glacial periods [*Jouzel et al.*, 2007; *Shackleton et al.*, 2000].

[3] The Mid-Brunhes interval between MIS 11 and MIS 9 is considered to be an unusual long warm period within the last 1.0 Ma [*Droxler and Farrell*, 2000]. This period displays long-lasting and perhaps intense warmth and is generally characterized by the highest sea level stands, unusual far poleward penetration of warm waters and the increase of carbonate accumulation on the seafloor. These characteristics give MIS 11 a unique climate exhibiting warm interglacial conditions for an interval of at least 30 ka, a duration twice as long as the most recent interglacial stages [*Loutre and Berger*, 2003; *McManus et al.*, 2003; *Desprat et al.*, 2005; *Loutre*, 2003]. The beginning of MIS 11 is characterized by the highest-amplitude deglacial warming of the past 5 Ma and is associated with higher sea levels than present, maybe +2, +7 or +20 m above mean level, as consequence of melting of the Greenland and West Antarctic ice sheets [*Bowen*, 2009]. The orbital conditions of interglacial MIS 11 were similar to those experienced during the Holocene. Both interglacials occurred in times when eccentricity was at its minimum, so that the amplitude of the precessional cycle was dampened. Accordingly, MIS 11.3

[1]Unidade Geologia Marinha, LNEG, Lisbon, Portugal.
[2]CIMAR Associated Laboratory, Porto, Portugal.
[3]Department of Environmental Chemistry, Institute of Environmental Assessment and Water Research, Barcelona, Spain.

Copyright 2011 by the American Geophysical Union.
0883-8305/11/2010PA001927

has often been considered a better analog for our current climate conditions than any other of the more recent interglacials [*de Abreu et al.*, 2005; *Droxler and Farrell*, 2000; *Loutre*, 2003; *Loutre and Berger*, 2003]. Both, the Holocene and MIS 11.3, are characterized by small amounts of continental ice [*Loutre and Berger*, 2003].

[4] High-resolution climate records are needed for the understanding of the climate processes occurring in the past. Recent studies on the EPICA Dome C (EDC) ice core have described the history of the Antarctic temperature and the atmospheric gas concentrations during the past 900 ka [*Jouzel et al.*, 2007; *Loulergue et al.*, 2008; *Lüthi et al.*, 2008] which are similar to the oscillations revealed in marine benthic oxygen isotopic records [*Jouzel et al.*, 2007; *Shackleton et al.*, 2000]. In this respect, the atmospheric CO_2 record during the glacial-interglacial cycles exhibits remarkable differences prior to and after MIS 11 [*Lüthi et al.*, 2008; *Siegenthaler et al.*, 2005] with lower CO_2 levels during the earlier warm phases.

[5] Marine sediment studies have shown that the western Iberian Margin is a strategic area both for allowing high-resolution record of the rapid climate variability as well as reflecting the influences of the processes that occurred both in the Arctic and Antarctica [*Shackleton et al.*, 2000]. The climatic variability of the last four climate cycles in this area has been described [see *de Abreu et al.*, 2003; *Desprat et al.*, 2007; *EPICA Community Members*, 2004; *Martrat et al.*, 2004, 2007; *Roucoux et al.*, 2006; *Tzedakis et al.*, 2003]. However, high-resolution marine data prior to MIS 11 or even for the complete deglacial transition from MIS 12 to 11 is lacking and that makes it difficult to understand the North Atlantic's response to Mid-Pleistocene climate variability.

[6] One of the major challenges in paleoclimate research is the study of past abrupt climate changes. The most extreme episodes noticed for the last glacial period are known as "Heinrich events" and were identified by the anomalous presence of ice-rafted detritus (IRD) transported to the North Atlantic, at latitudes between 40°N and 50°N, by icebergs drifting from the Northern Hemisphere ice sheets [*Bond et al.*, 1992, 1999; *Broecker*, 1994; *Hemming*, 2004]. Besides the IRD deposition, iceberg melting contributed to a substantial decrease in North Atlantic SST [*Cortijo et al.*, 1997]. These layers have also been detected further south, in the Iberian Margin [e.g., *de Abreu et al.*, 2003; *Bard et al.*, 2000; *Chapman et al.*, 2000; *Lebreiro et al.*, 1996; *Zahn et al.*, 1997]. Recently *Hodell et al.* [2008] have recognized Heinrich-like layers in the IRD belt (Site U1308) during previous glacial periods such as MIS 8, 10, 12 and 16. Yet, these layers have not been detected either during MIS 6, MIS 14 or during glacial periods prior to 640 ka or further south of the IRD belt.

[7] The aim of this work is, therefore, to understand the climate variability that occurred before and after the Mid-Brunhes event and, in particular, to explore how North Atlantic surface waters responded to pre-MIS 11 climate forcing, and if the frequency and amplitude of abrupt climate events were similar in their general trends to those occurring during the last glacial period. For this, we have performed the first high-resolution (centennial-scale) biomarker-based climate reconstruction of core MD03-2699 from the western Iberian Margin. The proxies analyzed provide information on the past hydrographic conditions such as SST, productivity determined from total organic carbon (TOC) and alkenone concentrations, and transport of terrestrial markers to this hemipelagic site.

2. Modern Hydrologic Conditions

[8] The MD03-2699 deep-sea core was recovered from the western Iberian Margin (39°02.20′N, 10°39.63′W; Estremadura spur) at about 100 km offshore and from 1895 m water depth (Figure 1a). This region is at present dominated by the surface Portugal Current System (PCS), the eastern recirculation of the North Atlantic's subtropical gyre [*Fiúza*, 1983; *Peliz et al.*, 2005], which is composed of a slow equatorward current in the open sea and a fast, seasonally reversing, coastal current [*Ambar*, 1994]. The Portugal Current (PC) advects freshly ventilated surface and subsurface waters slowly southward. During winter, waters from the eastern branch of the subtropical Azores Current recirculate northward along the western Iberian Margin as the Iberian Poleward Current (IPC) (Figure 1b) [*Peliz et al.*, 2005]. Coastal upwelling of subsurface cold and nutrient-rich waters occurs between May and September as a response to the strong northerlies [*Fiúza et al.*, 1982]. Under these conditions, upwelling filaments are observed off Peniche and Cape Roca [*Fiúza et al.*, 1982].

3. Material and Methods

[9] Core MD03-2699 was retrieved using a giant CALYPSO piston corer during the PICABIA oceanographic cruise on board the R/V *Marion Dufresne II*. This sedimentary record, mainly composed of hemipelagic silty clays, is 26.56 m long, and covers the last 580 ka (MIS 15 to 1). In this study, we will focus on the periods covering MIS 15–9 (580–300 ka) and MIS 1 (15–0 ka).

[10] Alkenones were used to reconstruct past SST ($U^{k'}_{37}$ index), productivity and the possible advection episodes of subpolar water masses, reflected by the relative proportion of the tetraunsaturated alkenone ($C_{37:4}$) to total C_{37} alkenone concentration, considering that $C_{37:4}$ is indicative of cold surface waters, especially in conjunction with increased meltwater input and thus reduction in surface water salinity [*Bard et al.*, 2000; *Cacho et al.*, 2001; *Rosell-Melé et al.*, 1998; *Villanueva et al.*, 1997a]. To reconstruct the terrigenous input higher plant biomarkers, such as odd carbon numbered C_{27}–C_{31} n-alkanes and even carbon numbered C_{22}–C_{30} alkan-1-ols, were quantified.

[11] The analytical procedure for determining the organic biomarkers is described in detail elsewhere [see *Villanueva et al.*, 1997b] and was performed in the laboratory of IDÆA-CSIC, Barcelona. Sediment samples were freeze-dried and the organic compounds were extracted by sonication using dichloromethane. The extracts were digested with 6% potassium hydroxide in methanol to eliminate interferences from wax esters, proteins and other hydrolysable compounds. The neutral lipids were extracted with hexane, evaporated to near dryness under a N_2 stream and finally derivatized with bis(trimethylsilyl)trifluoroacetamide. They

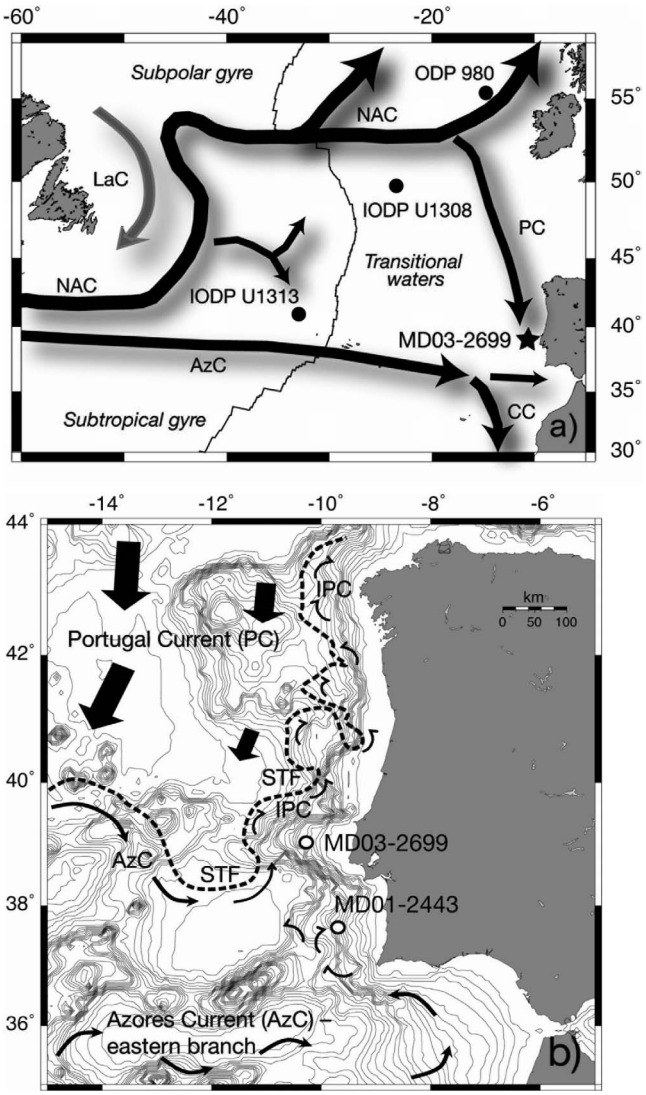

Figure 1. (a) Maps showing the core locations MD03-2699 (this study), ODP 980 [*McManus et al.*, 1999], and IODP U1313 [*Stein et al.*, 2009] and major surface water currents in the North Atlantic: GS, Gulf Stream; NAC, North Atlantic Current; AzC, Azores Current; CC, Canary Current; PC, Portugal Current; LaC, Labrador Current. (b) Close-up of Iberian Margin circulation after *Peliz et al.* [2005] (with permission from Elsevier) with IPC, Iberian Poleward Current, and STF, Subtropical front (adapted from *Voelker et al.* [2009]). The Iberian Margin sediment cores mentioned in the text. The core studied MD03-2699 (39°02.20′N, 10°39.63′W at −1865 m below sea level). Relevant paleoarchive of the MD01-2443 (37°52.85′N, 10°10.57′W, 2925 m below sea level).

were then analyzed with a Varian Gas chromatograph Model 3400 equipped with a septum programmable injector and a flame ionization detector. Selected samples were examined by gas chromatography coupled to mass spectrometry for confirmation of the GC peak assignments. A small (30) number of samples were analyzed at the biogeochemistry lab of the Marine Geology Unit (UGM) of LNEG, after a rigorous calibration of the new Varian Gas chromatograph Model 3800 equipped with a septum programmable injector and a flame ionization detector. The comparison of the obtained results from the two laboratories has shown deviations of less than 0.5°C. This value is included in the error bars of the method as previously suggested by *Grimalt et al.* [2001]. Transformation of $U^{k'}_{37}$ indices into SST was performed using the global core top calibration of annual SSTs [*Müller et al.*, 1998].

[12] TOC was determined on aliquots (2 mg) of dried and homogenized sediment samples collected at the same levels as those used for biomarker determination. TOC was analyzed in ground sediment with the UGM-LNEG CHNS-932 Leco elemental analyzer using the difference between total and inorganic carbon. The relative precision of repeated measurements of both samples and standards was 0.03 wt %.

[13] The abundance of lithic fragments, reflecting IRD deposits, was determined in the sediment fraction >315 μm. Benthic δ^{18}O analyses was performed in the epibenthic *C. pachyderma* or *C. wuellerstorfi* specimens from the same sediment fraction at MARUM (University Bremen, Germany) using a ThermoFinnigan MAT 252 mass spectrometer. The mass spectrometer is coupled to an automated Kiel carbonate preparation system and the long-term precision is ±0.07‰ for δ^{18}O.

4. Chronostratigraphy

[14] The benthic δ^{18}O record of core MD03-2699 reflects fluctuations between the prevailing deep water masses, i.e., North Atlantic Deep Water (NADW), Glacial North Atlantic Intermediate Water (GNAIW) and Mediterranean Outflow Water (MOW) [*Voelker et al.*, 2007], and sometimes greatly deviates from the global stack LR04 (Figure 2). Thus for establishing the age model we chose to correlate the MD03-2699 record with the intermediate-depth record of ODP Site 980 [*Flower et al.*, 2000; *McManus et al.*, 1999; *Oppo et al.*, 1998] retrieved from the Feni Drift at 55°N from 2168 m water depth. To maintain the link to the LR04 stack we used the ODP Site 980 record on its LR04 chronology [*Lisiecki and Raymo*, 2005]. Both the MD03-2699 and ODP Site 980 records were directly correlated by using primary control points between the two benthic δ^{18}O curves (Figure 2 and Table 1). Subsequently, small adjustments in the sedimentation rates resulting from the primary control points were made by aligning local maxima and minima values (Figure 2). Within the interval between 524 to 493 ka no clear benthic signals were found, so that the age control point here was added based on the *G. inflata* record [*Voelker et al.*, 2009]. We assume that the warming in the surface waters at the end of MIS 13.2 should be contemporaneous in the different sites from the midlatitudes North Atlantic Ocean and therefore the *G. inflata* δ^{18}O signal from core MD03-2699 could be directly correlated to that from the IODP Site U1313 [*Voelker et al.*, 2009].

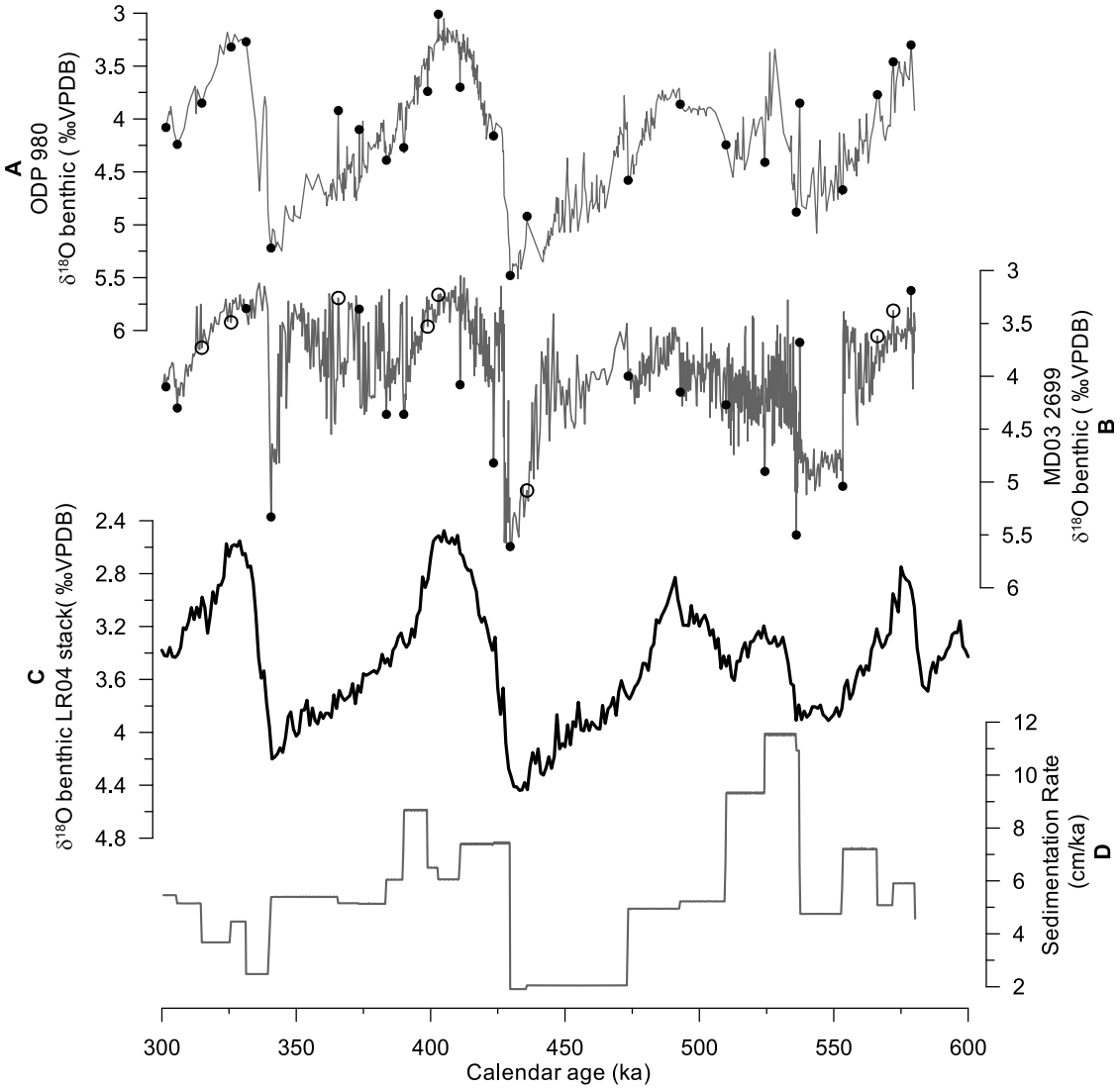

Figure 2. Records used for reconstructing the age model at site MD03-2699 from 580 to 300 ka. (a) The benthic δ^{18}O of the North Atlantic sediment core ODP980 [*McManus et al.*, 1999] on LR04 chronology. (b) Benthic δ^{18}O MD03-2699 (this study). (c) Benthic δ^{18}O profile of LR04 stack [*Lisiecki and Raymo*, 2005]. (d) Sedimentation rate of the core MD03 2699. Solid dots mark the primary control points, and the open circles mark the alignments according to Table 1.

[15] The age model thus obtained is supported by three nannofossil biostratigraphic events. The last common occurrence of *Pseudoemiliana lacunosa* was observed at 1895 cm (F. O. Amore et al., Coccolithophore record during the middle Pleistocene in the North Atlantic: Paleoclimatic and paleoproductivity patterns, submitted to *Marine Micropalenotology*, 2010). Our age model shows that this depth corresponds to an age of about 452.5 ka, being therefore in agreement with the age limits proposed by *Raffi et al.* [2006] for the presence of this specimen. Also, the abundance increase of *Gephyrocapsa caribbeanica* was detected at 2450 cm in core MD03-2699 at 546.4 ka being therefore in agreement with the timing of expansion of this species suggested by *Baumann and Freitag* [2004] and *Flores et al.* [2003]. Last, the first occurrence of *Helicosphaera inversa* was determined at 2170 cm which corresponds to an age of 514.9 ka (Amore et al., submitted manuscript, 2010).

[16] In this study, we focus on the core sections covering MIS 1 (15–0 ka) and MIS 15 to MIS 9 (580 to 300 ka) involving sedimentation rates between 11.5 cm/ka and 1.9 cm/ka in the deeper part of the record (Figure 2). Lowest rates are associated with the glacial periods when the MOW as stronger bottom current caused some winnowing.

[17] The age model of the last 23 ka, i.e., the upper 3 m of the core, is based on AMS ^{14}C dates [*Rodrigues et al.*, 2010] and the correlation of the MD03-2699 SST record with that of core MD01-2444 [*Martrat et al.*, 2007]. Sedimentation

Table 1. Age Model for Core MD03-2699

Depth (cm)	Age (ka)	Comment
1135	301.54	primary control point
1158	305.75	primary control point
1205	314.88	alignment
1245	325.76	alignment
1270	331.36	primary control point
1293	340.64	primary control point
1428	365.66	alignment
1468	373.42	primary control point
1520	383.55	primary control point
1559	390	primary control point
1636	398.87	alignment
1662	402.87	alignment
1711	410.96	primary control point
1803	423.4	alignment of minima
1849	429.6	primary control point
1861	435.87	alignment
1938	473.48	primary control point
2034	492.88	primary control point
2123	509.9	primary control point based on *G. inflata* records
2258	524.37	primary control point
2393	536.06	primary control point
2407	537.34	primary control point
2483	553.33	primary control point
2576	566.24	alignment
2606	572.14	alignment
2645	578.74	primary control point

rates were in the order of 10 cm/ka allowing an average resolution of 168 years for the 2 cm sampling interval.

5. Results

5.1. Sea Surface Temperature Variability

[18] The alkenone-derived SST record of core MD03-2699 shows that temperatures varied from 8°C to 20°C, between 580 and 300 ka, in the midlatitudes of the eastern North Atlantic (Figure 3). The warmest temperature values were detected during the climatic optimum of MIS 9 (at MIS 9.3) and the coldest at the end of MIS 12 during Termination V (Figure 3e). In general, the increase of SST during interglacials is synchronous with the northern latitude ice sheets' retreat as demonstrated by the lower $\delta^{18}O$ values in the LR04 benthic stack (Figures 3e and 3i). In contrast, during glacial periods the SST profile often exhibits much warmer values than expected when compared to the expansion of the northern ice sheets (Figures 3e and 3i). Extreme cold conditions occurred preferentially during both the pleniglacial and glacial inceptions and during the first phase of Terminations V and IV (Figure 3e). The second phase of Terminations V and IV are marked by a sharp SST increase (9°C and 8°C, respectively) while Termination VI is characterized by a smooth rise in temperatures (2°C).

5.1.1. Interglacial Periods

[19] A gradual long-term increase of the average SSTs (16°C to 17°C and 19°C) is detected during the warmest phases of the interglacial periods of MIS 13, 11 and 9, respectively (Figure 3e). In contrast, the duration of optimum interglacial conditions became shorter from MIS 13 to MIS 11 and finally to MIS 9 (Figure 3e). The MIS 13.1 optimum lasted 34.7 ka (514.7 to 480.06 ka), the MIS 11.3 one 30.7 ka (426.6 to 395.9 ka) and the MIS 9.3 one 20 ka (336.2 to 316.2 ka) (Figure 3e).

[20] The entire MIS 13 was a long, relatively stable period of 61 ka (534.5 to 478.7 ka) with average SST values around 16°C, however during MIS 13.1 and MIS 13.3 they reached 17°C.

[21] The interglacial MIS 11.3 was also a long warm period, from 426.6 to 395.9 ka with SST varying between 16.5°C and 18.5°C (Figure 3e). In close-up, this interglacial is actually subdivided into three phases: two warm SST plateaus separated by a rapid relative cold episode. Mean SST values of 18°C, occurring between 426.4 and 415.4 ka, characterized the first warming phase. During the second phase the SST dropped down to 16.5°C at 412.7 ka. Finally, an increase of SST up to 18°C occurred between 410.8 and 397.7 ka during the third phase of MIS 11.3 (Figure 3e).

[22] MIS 9.3 is the warmest period detected in the studied interval and is characterized by SST values of about 19°C (Figure 3e). This interval shows, a decreasing trend to 16°C at the end of MIS 9. The optimum SST conditions in western Iberia occurred during the retreat of the Northern Hemisphere ice sheets. However, sea surface maximal warming leads the maximum ice retreat by some ka during the last two interglacial periods (MIS 11 and MIS 9) (Figures 3e and 3i).

5.1.2. Abrupt Climate Variability

[23] Extreme cooling of about 4°C–7°C was detected during glacial periods and glacial inceptions, e.g., MIS 14, MIS 12 and MIS 10 (Figure 3e).

[24] The transition between MIS 15.1 and MIS 14 (567.1 ka–563.7 ka) is marked by an abrupt SST cooling of 5°C. After this extreme cooling, SST increased up to 17°C and dropped down again to 14°C between 562 ka and 555 ka. Following a SST increase at 550.5 ka the SST

Figure 3. Comparison between the MD03-2699 Iberian record and others to other climate records from 580 ka to 290 ka. (a) Daily insolation at 65°N during the summer solstice [*Berger*, 1978]. (b) The ODP-980 relative proportion of ice-rafted detritus (IRD) >150 μm record events when the ice shelves reached a critical extension [*McManus et al.*, 1999]. (c) The MD03-2699 relative proportion of IRD >315 μm (this study). (d) The percentage tetraunsaturated alkenone ($C_{37:4}$) to total alkenones is indicative of Arctic surface waters of MD03-2699 (this study). (e) $U^{k'}_{37}$-sea surface temperature in a core MD03-2699 with the interstadial events number on top and the stadials on bottom. The gray bars show the transitions between glacial and interglacial periods (terminations/deglaciations), the dashed lines mark abrupt SST decreases, and the blue bands mark Heinrich-type ice-rafting events. (f) $U^{k'}_{37}$-SST in IODP Site U1313 (41°N) from 470 to 310 ka [*Stein et al.*, 2009]. (g) The percentage of Polar planktic foraminifera species *N. pachyderma* (s.) at ODP Site 980 [*Oppo et al.*, 1998]. (h) Planktonic $\delta^{18}O$ (‰VPDB) of ODP Site 980 [*McManus et al.*, 1999]. (i) Benthic $\delta^{18}O$ LR04 stack [*Lisiecki and Raymo*, 2005]. (j) The temperature (°K) profile from the EPICA Dome C ice core [*Jouzel et al.*, 2007].

declined to 14°C during the glacial maximum of MIS 14.2. The transition of MIS 14 to MIS 13 (at around 533.4 ka) is marked by a SST increase of about 3°C (attaining up to 17°C during MIS 13.3) in 5 ka (539.5–534.5 ka). During the glacial inception into MIS 12, the SST decreased 5°C from 478 to 473.5 ka. A second cooling episode with temperatures close to 12°C occurred at 450 ka. Then, after a warming up to 16°C, SST dropped abruptly (during 3.7 ka) to 8°C at 427.9 ka (the coldest values recorded in the studied section of the core). The transition to the subsequent interglacial MIS 11 was been recorded by a SST increase from 8°C to 18°C in 2.4 ka (425.5–427.9 ka).

[25] The end of MIS 11.3 is also characterized by a SST drop of 4°C from 394.2 ka to 390 ka followed by a rapid increase back to 16°C at 388.6 ka. This warm episode, MIS 11.3, lasted 2.3 ka and ended in a strong cooling to 12°C at 383 ka (lasting 2.4 ka) followed by a rapid increase back to

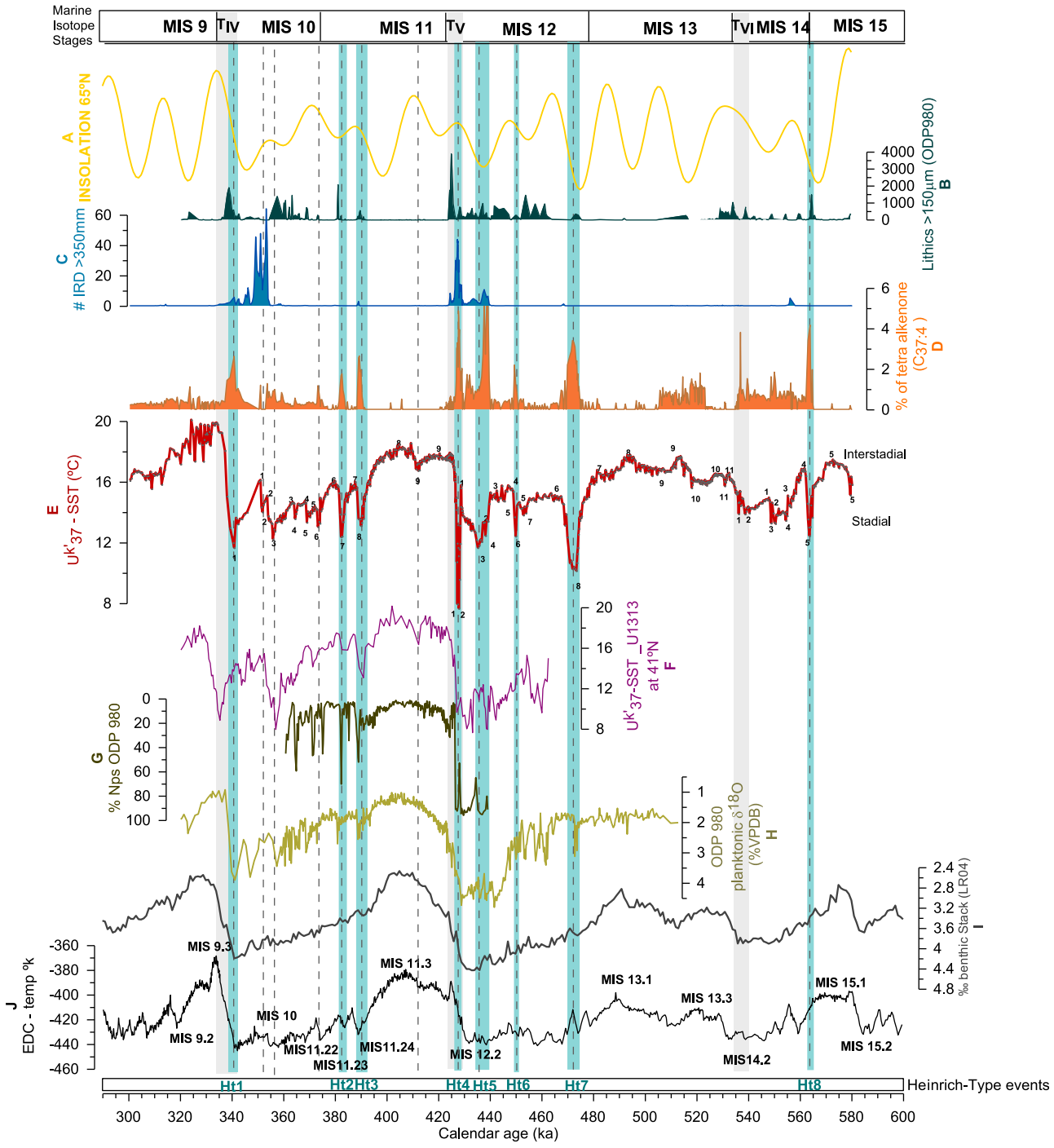

Figure 3

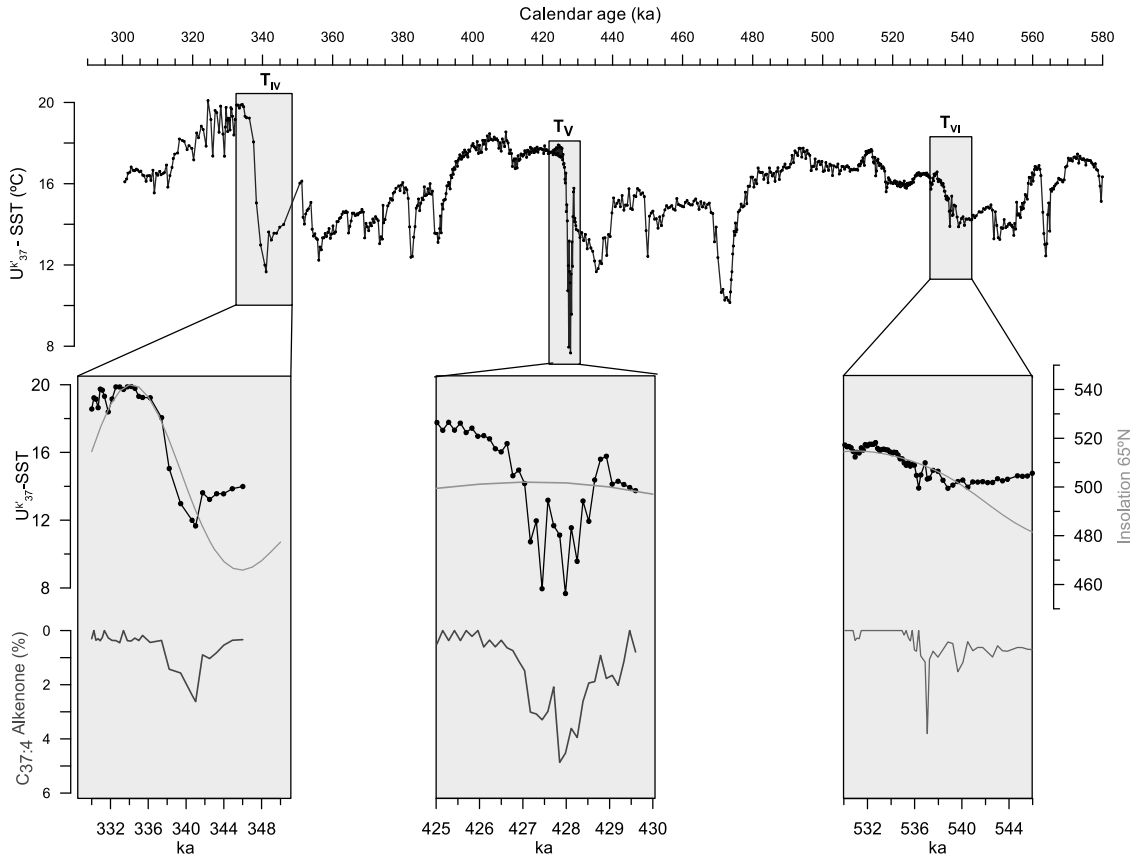

Figure 4. Close-ups of deglacial intervals associated with Terminations IV, V, and VI in the records of core MD03-2699, showing the $U^{k'}_{37}$-SST, the percentage of tetraunsaturated alkenone to total alkenones, and the daily insolation at 65°N during the summer solstice [*Berger*, 1978].

16°C at 381.1 ka (within 1.9 ka). This glacial inception was marked by an additional SST drop to 13°C at 374.2 ka.

[26] The final transition into MIS 10 is characterized by an interval of time around 12.3 ka with SST close to 14°C and variations of about 1°C (374–356 ka; Figure 3e). Then, there is a SST increase up to 16°C at 351.2 ka and a drop to 11.7°C during the glacial maximum at 341.6 ka. The transition to MIS 9 involved a SST increase from 12°C to 19°C (close to the maximum values characterizing the interglacial period) between 340.6 ka and 336.2 ka (Figure 3e). The interglacial period was marked by rapid SST oscillations of 2°C (Figure 3e). MIS 9.2 is recorded by a drop of 2°C between 317 ka and 313.5 ka followed by an increase of SST up to 17°C which lasted for 10 ka.

5.2. Advection of Subpolar Water Masses

[27] The advection of subpolar water masses can be identified by low SST values, high percentages of heptatriatetraenone ($C_{37:4}$) and high ice-rafted detritus abundances. Indeed, studies performed in more recent periods in both the western Iberian Margin and the Alboran Sea have shown that low SST values were associated with high percentages of $C_{37:4}$ and that SST minimum values were connected to episodes of subpolar waters arrival into those regions [*Bard et al.*, 2000; *Cacho et al.*, 1999; *Martrat et al.*, 2004, 2007]. Others have shown that the presence of IRD in western Iberian Margin sediments during the last glacial period was associated with the southward displacement of the Polar Front down to the midlatitudes of the North Atlantic favoring therefore the arrival of subpolar water masses into that region [e.g., *de Abreu et al.*, 2003; *Eynaud et al.*, 2009]. Our record also shows that the high percentages of $C_{37:4}$ occurred synchronously with low SST values (Figures 3e and 4) during Terminations IV, V and VI and during glacial inceptions (Figure 4). The highest percent of $C_{37:4}$ are detected during the extreme cold episodes of MIS 12. Episodes of high $\%C_{37:4}$ are also observed in the cold phases of MIS 14 and in the two cooling events of MIS 11 (Figure 3d).

[28] During most of the interglacial warm periods the concentrations of $C_{37:4}$ were negligible with the exception of a long section of MIS 13 (Figure 3d). This suggests that the arrival of subpolar waters off western Iberia occurred preferentially during the cold phases of the MIS 15–MIS 9 interval.

[29] Although the IRD abundance curve does not match perfectly with the SST and $\%C_{37:4}$ records they can provide some additional information in some cases (Figures 3d and 3e). The high IRD abundances occurred synchronously with high $\%C_{37:4}$ and low SST during part of MIS 12, especially

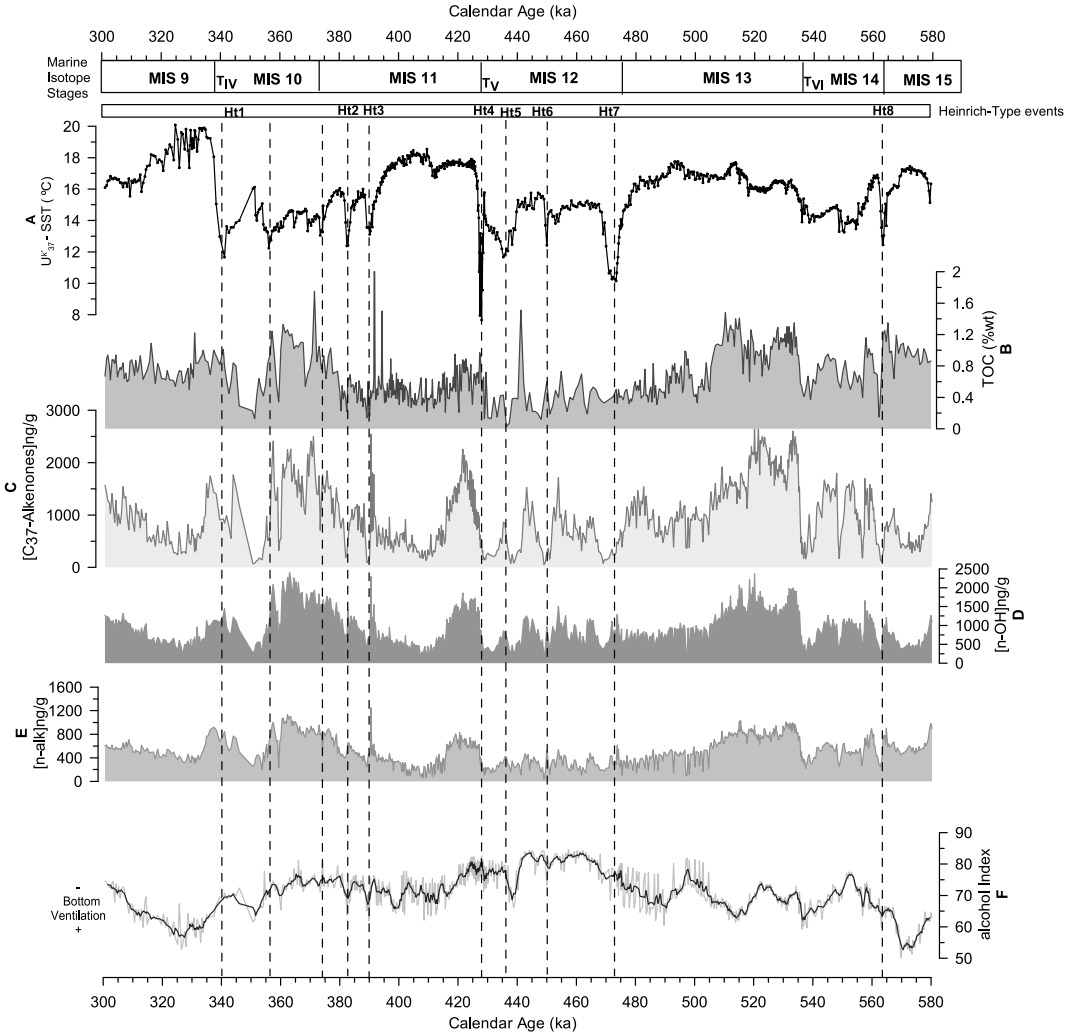

Figure 5. Results of organic matter content in the sediment core MD03-2699 (this study). (a) $U^{k'}_{37}$-SST. (b) The wt % of total organic carbon given a quantification of the organic matter in the site. (c) Total alkenone concentration (ng/g) of 37 carbon atoms reflect the coccolithophore productivity. (d) Concentration of total *n*-alkane-1ol (ng/g). (e) Concentration of total *n*-alkanes (ng/g). Figures 5d and 5e provide an estimation of the continental material that arrives to the site. (f) The relative proportion of *n*-hexacosan-1-ol (C_{26}OH) to the sum of *n*-hexacosan-1-ol (C_{26}OH) plus *n*-hexacosane (C_{29}) providing an oxygenation marker of the deep seafloor. The dashed lines mark abrupt SST decreases.

during Termination V (Figures 3c and 3d). In contrast, high IRD abundances occurred in the older phase of MIS 10, during the beginning of the SST decrease but not in parallel with the high $\%C_{37:4}$ (Figures 3d and 3e). The highest abundances of IRD occurred during Termination V synchronously with the most extreme sea surface cooling (Figures 3d and 3e). Although there is an extreme sea surface cooling during Terminations IV and VI, IRD was virtually absent (Figures 3d and 3e). The virtual absence of IRD during some extreme cold episodes does not signify that icebergs did not reach the western Iberian Margin. It could be possibly the result of the methodology employed here. IRD counting was performed in the >315 μm fraction rather than >150 μm, the standard size for semiquantitative IRD analysis [*Hemming*, 2004], or icebergs reaching the site had already lost their sediment load.

5.3. Variations in Concentrations of Terrigenous and Marine Biomarkers and of Organic Carbon Content

[30] The two terrigenous biomarkers, *n*-alkanes and *n*-akane-1-ols (Figures 5d and 5e), reveal the same variability, with a correlation coefficient of 0.77 in the MD03-2699 record. The highest concentrations of both proxies were detected during the MIS 13 and 10 but also being abundant at the beginning of MIS 13, 11 and 9.

[31] The concentrations of total C_{37} alkenones (Figure 5c) and TOC (Figure 5b), which are the common proxies used to quantify the marine productivity; follow the same patterns as the *n*-alkanes and *n*-akane-1-ols (Figures 5d and 5e). The

correlation coefficients between total C_{37} alkenones and *n*-alkane-1-ols and n-alkanes are 0.79 and 0.66, respectively. In general, the higher concentrations of organic biomarkers (close to 2500 ng/g for C_{37} alkenones and for *n*-akane-1-ols and 1200 ng/g for *n*-alkanes) were recorded during MIS 10 and during the first warm phases that followed the terminations (Figure 5). In general, there is no correspondence between changes in these proxies and the variability of the n-hexacosan-1-ol index (Figure 5f) indicating that the observed variations in the markers of terrigenous and marine origin were not related to changes in the bottom water ventilation. The longest periods with high values of both terrigenous and marine productivity proxies occurred during MIS 13 and 10, encompassing interglacial and glacial stages, respectively.

[32] Abrupt variability is also recorded in the profiles of C_{37} alkenones, *n*-alkan-1-ols and *n*-alkanes. SST drops are generally coincident with rapid concentration decreases of these proxies (Figures 5a, 5c, 5d, and 5e).

6. Discussion

6.1. Rapid Climate Changes and Surface Water Mass Variability

[33] The periods covering the MIS 15–MIS 9 (580–300 ka) and the MIS 1 (15–0 ka), recorded in core MD03-2699, are characterized by a general trend of warm and relative stable interglacial periods which contrast with high-frequency variability during glacial inceptions and glacials (Figure 3). The transition from relatively stable interglacials to unstable glacial conditions occur when the benthic threshold value for ice sheet instability was passed, coinciding with the increase of continental ice volume [*McManus et al.*, 1999], higher-amplitude changes in Antarctica, and decrease of greenhouse gas concentrations (Figures 3 and 6).

[34] Superimposed on the glacial-interglacial oscillations, suborbital millennial-scale climate variability was detected in the western Iberian Margin (Figure 3). Thus, we have identified 21 cold, stadial-type SST oscillations. Five occurred during the interval from MIS 15.1 to MIS 14, eight during MIS 13–MIS 12 and finally, eight during MIS 11–MIS 10 (Figure 3e), suggesting that the SST shifts were more frequent during the more recent climatic cycles (Figure 6). Some of these events were extremely cold and probably associated with episodes of iceberg melting in the western Iberian Margin, as demonstrated by the extreme cold SST values, the highest tetraunsaturated alkenone percentages and sometimes by the presence of IRD rich layers in core MD03-2699 (Figures 3c, 3d, and 3e). These events are similar in their general trends to those detected in the midlatitudes of the eastern North Atlantic during the last glacial period, known as Heinrich events [*de Abreu et al.*, 2003; *Bard et al.*, 2000; *Eynaud et al.*, 2009; *Martrat et al.*, 2007; *Naughton et al.*, 2009; *Pailler and Bard*, 2002; *Voelker et al.*, 2006]. We therefore associated the extreme cold phases occurring between 580 and 300 ka (MIS 15–9) with Heinrich-type events. It is also known that during Heinrich events extreme SST coolings and reduction in Atlantic Meridional Overturning Circulation (AMOC) favored the southward displacement of the Polar Front down to the midlatitudes of the North Atlantic [*López-Martínez et al.*, 2006; *Naughton et al.*, 2009; *Voelker et al.*, 2006; *Eynaud et al.*, 2009].

[35] Regarding in detail alkenone-based SST records from the western Iberian Margin (MD01-2444 [*Martrat et al.*, 2007]; MD95-2042, MD95-2040 [*Pailler and Bard*, 2002]; and MD99-2331 [*Naughton et al.*, 2009]) that cover the last glacial period we observe a gradual pattern of SST decrease from south to north during Heinrich events. *Salgueiro et al.* [2010] based on foraminifera-derived summer SST, also detected the same latitudinal gradient pattern along the Iberian Margin and demonstrated that the northern Iberian Margin was more affected by the subpolar water masses than the southern part which was more influenced by the subtropical water masses from the Azores current. Core MD03-2699 is located at or close to the boundary between these areas and being affected by both water masses. The study area is therefore highly sensitive to the water mass fluctuations and changes in the position of the subtropical and subpolar hydrographic fronts that occurred in the past.

[36] We identified eight Heinrich-type (Ht) events between 580 and 300 ka (MIS 15–9) in core MD03-2699 (Figure 3). Ht8 was detected during the glacial inception of MIS 14 and is marked by a drop of SST down to 12°C (reaching values colder than those recorded during the glacial MIS 14) and high percent of $C_{37:4}$ (Figures 3d and 3e). This suggests that during this event the Polar Front reached the southern Iberian Margin favoring the advection of subpolar waters into the study area. Ht7 (within MIS 12) was the coldest event detected within pleniglacial periods and shows high $\%C_{37:4}$ (Figure 3) suggesting therefore that the studied area was mainly under the influence of subpolar waters. During Ht6 (within MIS 12), the subtropical water masses had, probably, a strong influence on the site because the SST were not as cold and the $\%C_{37:4}$ not so high as that characterizing the previous Ht events (Figure 3). The core site also seems to have been highly influenced by the subpolar waters during Ht5 (MIS 12.2). Ht4 is the most extreme cold event detected between MIS 15 and MIS 9 and occurred at the beginning of Termination V (Figure 3). This event is however, complex and composed of three phases: two coolings separated by a warming (Figure 4). The first phase is marked by a drastic SST drop and, extremely high percentages of $C_{37:4}$; the second by an increase of SST of about 4°C and a decrease of $\%C_{37:4}$ and the third phase is characterized by the returning to cold conditions, high $\%C_{37:4}$ and high IRD content. This suggests that during both the first and third phases of Ht4 the Polar Front was probably displaced south of 39°N and therefore the studied area was mainly under the influence of the subpolar water masses and, that during the second phase of Ht4 the Polar Front was slightly displaced further north. A similar complex pattern was recorded in the Iberian Margin during extreme cold events within the last glacial period and last glacial-interglacial transition [*Bard et al.*, 2000; *Martrat et al.*, 2007; *Naughton et al.*, 2009; *Rodrigues et al.*, 2010; *Voelker et al.*, 2006] being associated to changes in the position of the Polar Front. During Ht3 and Ht2 (within the glacial inception of MIS 10) the subtropical water masses probably affected the

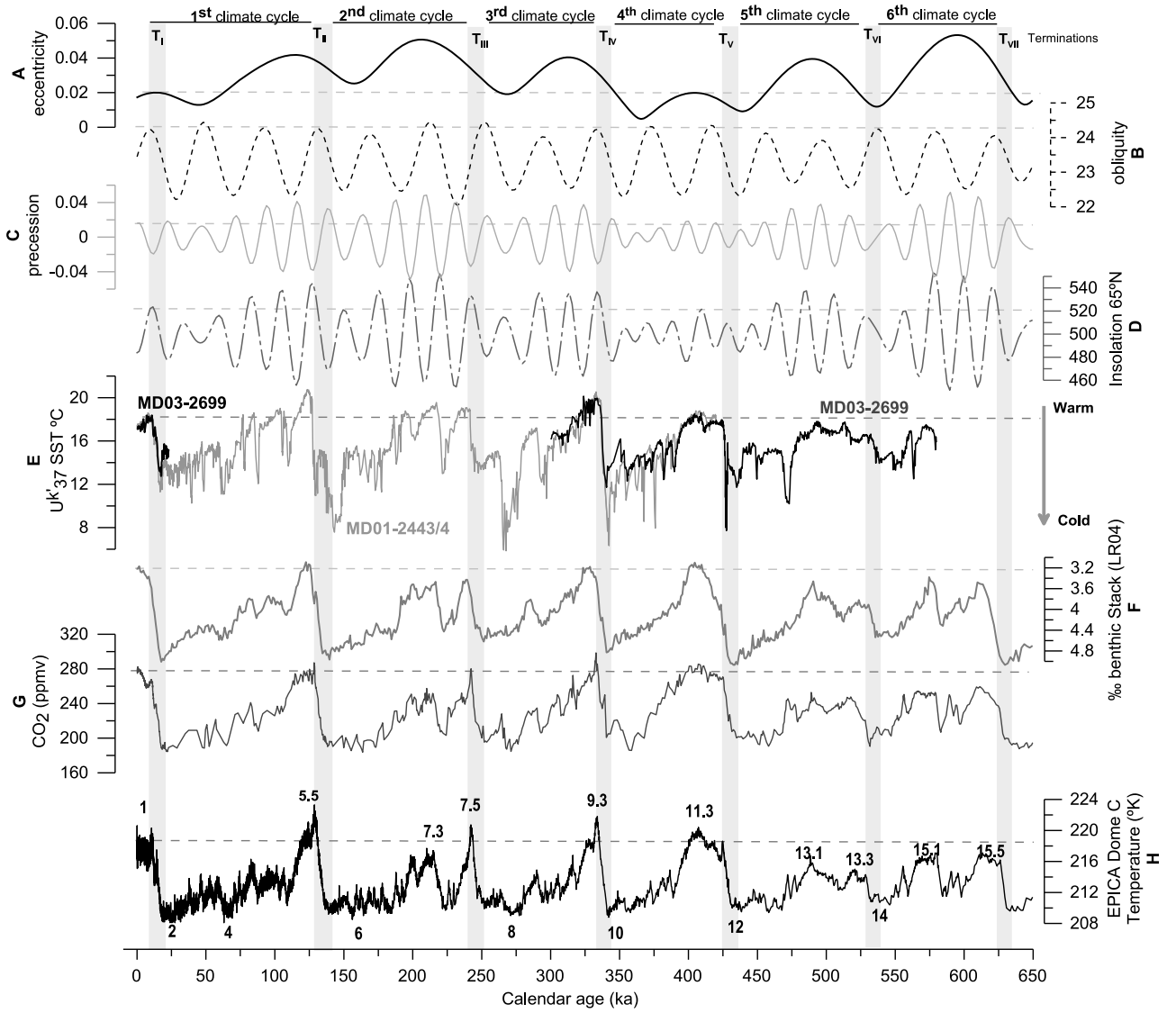

Figure 6. Iberian Margin sea surface record for the last 580 kyr in comparison to paleoarchive records over the last six climate cycles. (a) The eccentricity, (b) the obliquity, and (c) the precession of the Earth's orbit [*Berger*, 1978] are external triggers of the climate system. (d) Daily insolation at 37°N during the summer solstice. (e) Spliced alkenone-based SST records of cores MD01-2443 and MD01-2444 [*Martrat et al.*, 2007] and of core MD03-2699 (this study). (f) Benthic δ^{18}O LR04 stack [*Lisiecki and Raymo*, 2005]. (g) EDC CO_2 greenhouse gas concentrations [*Siegenthaler et al.*, 2005]. (h) Temperature (°K) profile of the EPICA Dome C ice core (EDC) [*Jouzel et al.*, 2007] with the marine isotopic stages (MIS). Gray bands mark terminations, and the dashed horizontal lines indicate Holocene levels.

hydrological conditions at the study site again as cooling was less pronounced. Finally, the youngest Ht event recorded in core MD03-2699, is Ht1. This event occurred during Termination IV and is marked by a SST decrease down to 12°C, moderate percent of $C_{37:4}$ and virtual absence of IRD (Figures 3 and 4). This suggests that besides the influence of subpolar water masses, as revealed by the $\%C_{37:4}$, the studied area was probably also affected by the advection of subtropical water masses.

[37] Similar events, characterized by the deposition of high quantities of IRD, were identified in the IODP Site U1313 record, based on the dolomite content analysis (reflecting a Canadian source of icebergs) [*Stein et al.*, 2009]. However, it is possible that some of these Heinrich type layers had a main contribution from the European ice sheets rather than the Laurentide ice shield [*Stein et al.*, 2009]. Two of these Heinrich-type episodes, identified in the Iberian Margin record (MD03-2699) as Ht2 and Ht3, coincided with two extreme events, marked by IRD peaks and extreme sea surface coolings (% *N. pachyderma* peaks), noticed for ODP Site 980, located close to the British ice sheet (Figures 1 and 3d) [*McManus et al.*, 1999; *Oppo et al.*,

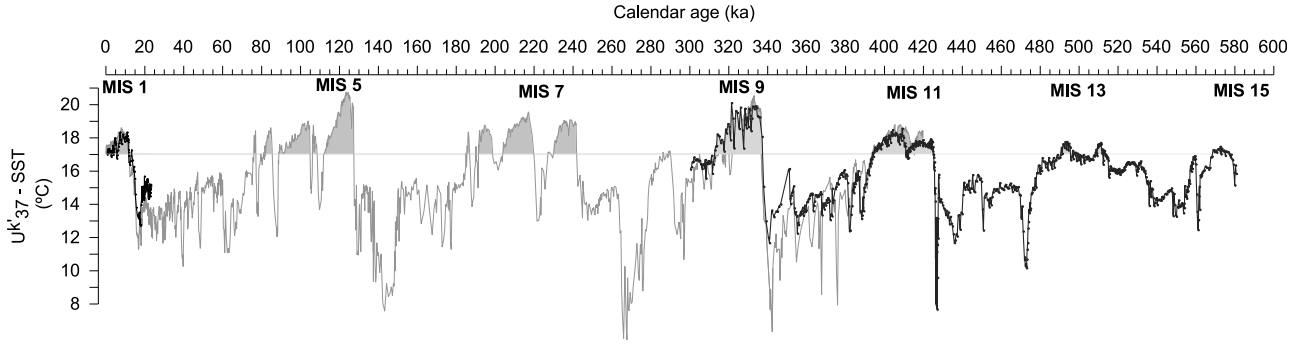

Figure 7. Zooming in the Iberian Margin alkenone-based SST records for the last 600 ka. Direct comparison of the interglacial temperature profiles.

1998]. These episodes occurred also in synchrony with episodes of substantial iceberg discharges recorded at IODP Site U1308 (Figure 1), also located close to the British ice sheet [*Hodell et al.*, 2008]. Far away from the British ice sheet, IODP Site U1313 [*Stein et al.*, 2009] (Figure 1) did not detect the presence of IRD layers during Ht2 and Ht3. Thus, only the records located next to the British ice sheets are characterized by IRD deposition, suggesting that the British ice sheet was probably the main source of IRD and freshwater during the Ht2 and Ht3. One additional Ht event than those recorded in core MD03-2699 was detected in IODP Site U1313 at around 355 ka [*Stein et al.*, 2009], but it did not have a great impact on the SST decrease in the western Iberian Margin.

[38] Ht events are also imprinted in the continental biomarkers records of MD03-2699 between MIS 15 and MIS 9 (Figures 5d and 5e). During most of the Ht events (Ht7 to Ht1), the terrigenous biomarkers' concentrations were very low (Figures 5d and 5e). The decrease of terrigenous biomarkers concentrations in marine sediments can be due to (1) changes in the prevailing wind patterns from easterlies to westerlies which preclude the transfer of cuticles from vascular plants to the sea and/or (2) temperate forest contraction in the neighboring continent. It is known that during last glacial Heinrich events the westerly prevailing winds preclude the transfer of high quantities of sediment into the deep sea [*Sánchez Goñi et al.*, 2002]. One could speculate that those environmental conditions had also prevailed during the previous Ht events within the MIS 15–MIS 9 interval. Also, the decrease of terrigenous biomarkers concentrations during Ht3 and Ht2 in the western Iberian Margin were contemporaneous with the two episodes of temperate and humid forest reduction in the Iberian Peninsula over MIS 11.23 and 11.24 [*Desprat et al.*, 2007] and increase of ice volume as documented by the benthic $\delta^{18}O$ [*de Abreu et al.*, 2005; *Tzedakis et al.*, 2003].

[39] The marine productivity inferred from the total alkenones concentration and TOC content of core MD03-2699 was very low during most Ht events (Ht7 to Ht1) (Figure 5b). Reduced productivity was also noticed for the last glacial Heinrich events in the northwestern Iberian Margin [*Salgueiro et al.*, 2010] and in the open North Atlantic and Norwegian Sea [*Nave et al.*, 2007]. A contrasting pattern has been detected during Ht8 which reveals high concentration of continental biomarkers and substantial marine productivity (Figures 5b and 5c) suggesting that exceptional environmental conditions associated with prevailing easterlies favored the input of continental nutrients into the ocean.

[40] In order to compare the suborbital climate variability detected in core MD03-2699, between 580 and 300 ka, with that characterizing more recent climatic cycles we combine our SST-$U^{k'}_{37}$ data with that of MD01-2443 [*Martrat et al.*, 2007]. The spliced SST-$U^{k'}_{37}$ profile of cores MD03-2699 and MD01-2443 clearly shows that suborbital-scale climate variability occurred in the Iberian Margin as far back in time as the sixth Pleistocene climate cycle (Figures 6 and 7). The SST-$U^{k'}_{37}$ record of core MD03-2699 overlaps that obtained in core MD01-2443 between MIS 11 and the mid-MIS 9 (Figures 6 and 7) and extends it further back in time until the end of MIS 15. Both records show the same pattern during the overlapping period and similar SST values during interglacial optimums. However, they do not show either the same SST values or amplitude of SST fluctuations within MIS 10 and late MIS11 (Figure 6). SST was a few degrees colder and the amplitude of suborbital oscillations was higher in the southernmost core (MD01-2443) than in core MD03-2699. This suggests that site MD01-2443 might have experienced of stronger upwelling conditions reflected by colder SST than at site MD03-2699.

[41] The composed Iberian Margin SST record (Figures 6 and 7) reveals that colder SSTs were recorded during MIS 8 than during MIS 12, even though the ice volume was higher during the latter glacial. This composed record also shows that the pattern of the last deglaciation (two cold phases coincided with Heinrich event 1 and Younger Dryas separated by a warming episode, the Bølling-Allerød) also occurred during deglaciations of MIS 8 and MIS 6 (Figures 6 and 7). The abrupt climatic shifts of those deglaciations were likely the result of changes in the position of the Polar Front and can be traced back at least to Termination V. This suggests that the deglacial pattern changed after the Mid-Brunhes event, associated with variations in the climate forcing.

[42] Glacial MIS 14 was warmer (14°C) than any of the later glacials (Figure 6), in agreement with what has been recorded in other regions, such as in North Atlantic (ODP Site 982 [*Wright and Flower*, 2002]), the subtropical North

Atlantic (ODP Site 1058 [*Billups et al.*, 2006]), off northwest Africa (ODP Site 658 [*Eglinton et al.*, 1992]), the southeast Atlantic Ocean [*Chen et al.*, 2002], and the eastern equatorial Pacific (ODP Site 849 [*Mix et al.*, 1995]). *Voelker et al.* [2009] suggest that a different circulation pattern was probably in place during this glacial period and that the subtropical waters of the Azores current had a substantial influence on the Iberian Margin. Also, both the terrestrial input and marine productivity were higher and different from what has been recorded in other glacial periods (Figures 5c, 5d, and 5e) supporting the idea that different circulation patterns prevailed during MIS 14.

[43] The transition of MIS12 to MIS11 and MIS 10 to MIS 9 is very similar reflecting the increase in biomarker concentrations contemporaneous with warmer SST, especially during the deglaciation, followed by an abrupt decline during the warm conditions and a gradual increase to the next glacial period. The transition of MIS 14 to MIS 13 is similar in their general trends to MIS12-MIS11 and MIS 10-MIS 9 deglaciations, with an abrupt increase of biomarker concentrations during the termination. However, biomarker concentrations remained high during most of MIS 13 before declining early in MIS 12. During the later MIS 12 the biomarker concentrations and thus productivity oscillated, in a similar way as during MIS 14, but maxima of MIS 12 and 14 only reached values as high as the late MIS 13.1 and never those from MIS 10 (Figures 5c, 5d, and 5e). This clearly indicates that climatic conditions such as the wind conditions reflected by the terrigenous biomarkers were different prior and after the mid-Brunhes event. The high productivity during MIS 13, i.e., during 54 ka, and the SST values lower than the more recent interglacial periods, could help explain the lower atmospheric CO_2 concentrations during MIS 13, in particular because also the planktonic foraminiferal $\delta^{13}C$ data imply lower nutrient concentrations or high nutrient consumption (high $\delta^{13}C$ values [*Voelker et al.*, 2009]).

[44] In general, the total concentration of biomarker compounds in the marine sediments is characterized by low content during glacial periods and increased during the deglaciations (Figure 5).

[45] Within the chronological constraints the millennial-scale oscillations observed during glacials (MIS 14, 12 and 10) and glacial inceptions, appear to have counterparts in the EPICA δD record where the same number of cooling events for each glacial interval is also identifiable (Figures 3 and 6). However, event Ht8 was very likely contemporary with the subsequent Antarctic major warming event labeled 14.3 in the work by *Jouzel et al.* [2007] and not with the cold phase like it is with the current age model. If this is true, it is consistent—in agreement with the response of Ht 4 as well—with the last ice age observation for the Greenland interstadials duration being correlated with the Antarctica warming amplitude [*EPICA Community Members*, 2004].

6.2. Interglacial Climate Conditions

[46] Interglacial periods, i.e., MIS 9.3, MIS 11.3, MIS 13.3 and 13.1, are detected in the SST profile of core MD03-2699 (Figure 7). Interglacial MIS 9.3 is warmer than the present interglacial in agreement with what has been noticed in other records from the Iberian Margin [*Desprat et al.*, 2007; *Martrat et al.*, 2007] and by the EPICA ice core temperature record [*Jouzel et al.*, 2007]. Our SST record, however, also highlights that the interglacials prior to MIS 9.3 lasted longer and had more stable mean annual surface temperatures. Interglacials following Terminations IV and VI are marked by an abrupt SST increase which parallels the increase of Northern Hemisphere summer insolation while that of Termination V occurred during the maximum of insolation (Figure 4).

[47] MIS 13, was a long, relative warm period experiencing some small-scale oscillations and was 2°C colder than the subsequent interglacial period. The two more stable interglacial periods, marked by the absence of $C_{37:4}$ alkenones, lasted 5 ka and occurred during MIS13.3 (around 510 ka) and MIS 13.1 (around 495 ka). However, only small SST variations were recorded for a period of about 54 ka making MIS 13 the longest interglacial for the last 580 ka, at least on the Iberian Margin. MIS 13 is also characterized by relatively low $\delta^{18}O$ values indicating a lower sea level than during the subsequent interglacials and maximum $\delta^{13}C$ levels both at the surface and in the deep ocean [*Hodell et al.*, 2003; *Lisiecki and Raymo*, 2005]. In the Southern Hemisphere the existing data indicates cooler Antarctic temperatures [*Jouzel et al.*, 2007], lower CO_2 and CH_4 concentrations [*Lüthi et al.*, 2008; *Siegenthaler et al.*, 2005], and lower summer sea surface temperatures in the South Atlantic [*McClymont et al.*, 2005]. Conditions that coincided with extremely strong Asian, Indian and African summer monsoons, weakest Asian winter monsoon and lowest Asian dust and iron fluxes [*Guo et al.*, 2009]. Pervasive warm conditions were also evidenced by the records from the Asian monsoon zone [*Yin and Guo*, 2007] and the northern high-latitude regions [*de Vernal and Hillaire-Marcel*, 2008]. Accordingly, *Guo et al.* [2009] conclude that a strong asymmetry of hemispheric climates existed during MIS 13 with a warmer Northern Hemisphere and a cooler Southern Hemisphere. Nevertheless, our record in the Iberian Margin shows a MIS 13 cooler than the subsequent interglacials contrarily to this recent consideration (Figures 6 and 7).

[48] The warmest phase of MIS 11, MIS 11.3, lasted 30 ka on the Iberian Margin and was synchronous with the major forest expansion episodes documented for the northwestern Iberian Peninsula [*Desprat et al.*, 2005, 2007]. During this interval, maximum SSTs of 18°C were interrupted by a short cooling event (1°C) around 412 ka (Figure 3). A similar pattern was registered in core MD01-2443, south of MD03-2699, and at the midlatitude North Atlantic IODP Site U1313 (Figure 3). At the latter site the minimum between the two plateaus within MIS 11.3 occurred at 413 ka and was more pronounced probably due to more variable conditions in the western North Atlantic and admixing of subpolar surface waters at that time [*Stein et al.*, 2009; *Voelker et al.*, 2009]. On the other hand, IODP Site U1313 shows a temperature maximum of 19°C during MIS 11.3 related to the stronger influence of the Gulf Stream/North Atlantic Drift at the site.

[49] The pattern reflected by the terrigenous biomarkers during MIS 11, with maxima during the early phase, is

similar to the dust record off northwestern Africa, ODP Site 958 [*Helmke et al.*, 2008]. Thus, the strengthening of the trade winds over northwestern Africa occurred synchronously with the increase of terrestrial input in the western Iberian Margin suggesting also a strengthening of the westerly winds in that region. The strong northerly winds led to a higher nutrient availability, either through upwelling or as continental coastal input, and thus to an increase in coccolithophores production as reflected by the higher concentration of total alkenones during the early phase of MIS 11.3. The total biomarker concentration started to decline with the onset of the humid period in Africa, that is before the first SST plateau ended, indicating that the shift in atmospheric circulation over Africa also impacted Iberia.

[50] In general terms MIS 11.3 and MIS 9.3 show similar conditions, but a major difference is noted in the ventilation of the surface to subsurface water masses and their impact on the meridional overturning circulation [*Voelker et al.*, 2009]. This difference is corroborated by the MD03-2699's SST and biomarker signals during MIS 9.3 when productivity decreased earlier than in the previous interglacials (Figure 5). In detail, the MIS 9.3 SST record reveals a warmer interval at the beginning of the interglacial with temperatures close to 20°C, i.e., 2°C warmer than during MIS 11.3, followed by a decreasing trend associated with millennial-scale variability of 2°C in amplitude during the second half of MIS9.3 until 320 ka (Figure 7) and prior to the onset of the next glacial inception that started with stadial MIS 9.2. The productivity increase was contemporary with maxima in the terrigenous markers suggesting that, as during the early MIS 11.3, stronger winds and an additional supply of nutrients from the continent sustained the productivity near the studied site (Figure 4). The productivity patterns observed in core MD03-2699 differ from those recorded at IODP Site U1313, where productivity during interglacials was minimal and high during the glacial periods [*Stein et al.*, 2009] highlighting the different responses of open ocean productivity (U1313) and upwelling-related productivity (MD03-2699) to the respective climate forcing.

6.3. Holocene Versus MIS 11

[51] The parallelism of the climate evolution between MIS 11.3 and the Holocene is not straightforward and extrapolations of past to present conditions leads to different perspectives on the length of the current interglacial depending on which parameter is used for chronological alignment [*Tzedakis*, 2009]. Synchronization according to precession shows that the present day should be analog to MIS 11 at 398 ka [*Loutre and Berger*, 2003]. In contrast, synchronization based on obliquity, i.e., Terminations I and V, shows that present day would correspond to 407 ka in MIS 11 [*EPICA Community Members*, 2004; *Masson-Delmotte et al.*, 2006].

[52] In the composed Iberian SST records for the last sixth climate cycles (Figures 6 and 7) the warmer interglacials were MIS 5.5 (Eemian) with 21°C, followed by MIS 9.3 (20°C) and MIS 7.5 (19°C), while maximum temperatures during MIS 11.3 (18°C) were similar to SST values found for the Holocene (Figure 7). This observation is not surprising because the orbital parameters of MIS 11.3 and the present interglacial, the Holocene, are also rather similar. Eccentricity was at minimum during MIS 11 and in the Holocene while insolation at 65°N and precession were similar as well. Sea level reconstructions based on benthic $\delta^{18}O$ values suggest that sea level 410 ka ago was also at a level similar to the one reached 10 ka ago (Figure 6).

[53] Holocene maximum SST values, close to 19°C, occurred between 10.5 and 9.7 ka while the MIS 11.3 record reveals two warmer phases: the first with maximum SST close to 18°C (427 to 412 ka) and a second with temperatures close to 19°C (407 to 395 ka). Both periods display a SST decrease following the maximum temperature values. However, in the case of MIS 11 that decreases was interrupted by the second SST increase along with the sea level highstand. A long-term decrease of 1.5°C in SST, is also similar in both periods at the Estremadura site MD03-2699 implying that the SST record of the first part of MIS 11 (427 to 412 ka) and the last 10.5 ka record reflect similar hydrographic conditions during both periods. In terms of duration of the two interglacials, the fact that interglacial duration changed toward shorter periods after the Mid-Brunhes event prevents further estimations.

7. Conclusion

[54] Our results allowed the reconstruction of climate variability, surface oceanic circulation, productivity and wind conditions, in the western Iberian Margin between MIS 15 to MIS 9. This study extends the existing biomarker record of core MD01-2443 back in time to the sixth climatic cycle (580 ka). The new results for the period between 580 and 300 ka show a general trend of warm and relative stable interglacial periods and high-frequency variability during the glacial inceptions and glacials. The SST profile shows warmer interglacial conditions after the Mid-Brunhes event with a 2°C increase from MIS 13 to MIS 11.3 and MIS 9.3, respectively. However, in terms of duration interglacial periods were longer prior to the Mid-Brunhes event, with MIS 13 reflecting the longest relative stable period (54 ka length) of the last 580 ka. MIS 11.3 was recorded as a long warm period with SST close to 18°C, similar to the present interglacial, the Holocene. The warmest interglacial, MIS 9.3, shows a 15.8 ka interval with SST around 19°C, but the second half of this interglacial, after 329 ka, was marked by 2°C amplitude millennial-scale variability.

[55] The composed record (MD03-2699 and MD01-2443) of SST-$U^{k'}_{37}$ shows colder periods during MIS8 than during MIS 12, even though the ice volume was higher during the latter glacial.

[56] A change in the deglaciation pattern detected before and after Termination V can be likely the result of a change in the climate forcing after the Mid-Brunhes event. Moreover, the climatic conditions and namely the wind conditions reflected by the terrigenous biomarkers and the productivity were different prior to and after the Mid-Brunhes event.

[57] Our results also show that superimposed on the glacial-interglacial oscillations, suborbital millennial-scale climate variability occurred in the western Iberian Margin as far back in time as the sixth climate cycle. Thus, we have

identified 21 stadial-type SST oscillations. The most extreme coolings were associated with episodes of iceberg melting as demonstrated by the extreme cold SST values, the highest tetraunsaturated alkenone percentages and sometimes by the presence of IRD rich layers and were related to Heinrich-type events. We identified eight Heinrich-type events between 580 and 300 ka: Ht1 during MIS10.2; Ht2, Ht3 during the glacial inception of MIS 11; Ht4 at the onset of Termination V; Ht5 (MIS 12.2); Ht6 and Ht7 over the glacial inception of MIS 12; and Ht8 (MIS 15.1). Ht4 is the most extreme cold event and shows a complex pattern (two cold phases separated by a relatively warm phase) similar to some last glacial Heinrich episodes, that was associated to changes in the position of the Polar Front.

[58] The study area is highly sensitive to the water mass fluctuations and changes in the position of the subtropical and subpolar hydrographic fronts, during both the glacial and glacial inceptions. This variability is imprinted in the MD03-2699 SST record and is related to the southward and northward migration of the Polar Front. Thus, during most of the extreme cold episodes the Polar Front moved southward favoring the entry of subpolar water masses in the midlatitudes of the North Atlantic and therefore the reduction of the AMOC. Other Ht events were not so extreme and indicating an influence of the subtropical Azores Current at the study site.

[59] Also, during glacial MIS14, a retreat of the Polar Front led to the advection of subtropical water masses with temperate SST values suggesting a strong influence of the subtropical Azores Current.

[60] The mid-depth location of our core site did not allow us to study interhemispheric linkages but the sites to be drilled off Iberia in water depths deeper than 2000 m during one of the proposed IODP expeditions will hopefully solve this issue in the near future. Only then will we be able to place our findings for the intervals prior to the Mid-Brunhes event, especially during MIS 13, into a more global context.

[61] **Acknowledgments.** The Fundação para a Ciência e a Tecnologia through the PORTO (PDCT/MAR/58282/2004) and SEDPORT projects (PDCTM/40017/2003), postdoctoral (SFRH/BPD/21691/2005), and Ph.D. (SFRH/BP/13749/2003) fellowships funded A.V. and T.R. The Spanish Ministry of Science and Technology (REN2003-08642-C02-01) and support from the Consolider-Ingenio 2100 Project CE-CSD2007-0067 are also acknowledged. Coring of MD03-2699 was made possible through an European Access to Research Infrastructure grant. We thank IPEV, Yvon Balut, and the captain and crews of R/V *Marion Dufresne* for their support in retrieving the Calypso core. Special thanks go to Monika Segl (MARUM, University Bremen), the staff of the UGM lab, and C. N. Prabhu who provided the samples for the AMS ^{14}C dating in the upper section of core MD03-2699.

References

Ambar, I. (1994), Alguns aspectos da física do oceano, report, pp. 21–34, Fund. Calouste Gulbenkian, Lisbon. (Available at http://zircon.dcsa.fct.unl.pt/dspace/handle/123456789/196.)

Bard, E., F. Rostek, J.-L. Turon, and S. Gendreau (2000), Hydrological impact of Heinrich events in the subtropical northeast Atlantic, *Science*, *289*, 1321–1324, doi:10.1126/science.289.5483.1321.

Baumann, K.-H., and T. Freitag (2004), Pleistocene fluctuations in the northern Benguela Current system as revealed by coccolith assemblages, *Mar. Micropaleontol.*, *52*(1–4), 195–215, doi:10.1016/j.marmicro.2004.04.011.

Berger, A. L. (1978), Long-term variations of daily insolation and Quaternary climatic changes, *J. Atmos. Sci.*, *35*, 2362–2367, doi:10.1175/1520-0469(1978)035<2362:LTVODI>2.0.CO;2.

Billups, K., C. Lindley, J. Fisler, and P. Martin (2006), Mid Pleistocene climate instability in the subtropical northwestern Atlantic, *Global Planet. Change*, *54*(3–4), 251–262, doi:10.1016/j.gloplacha.2006.06.025.

Bond, G., et al. (1992), Evidence for massive discharges of icebergs into the North Atlantic Ocean during the last glacial period, *Nature*, *360*, 245–249, doi:10.1038/360245a0.

Bond, G. C., W. Showers, M. Elliot, M. Evans, R. Lotti, I. Hajdas, G. Bonani, and S. Johnson (1999), The North Atlantic's 1–2 kyr climate rhythm: Relation to Heinrich events, Dansgaard/Oeschger cycles and the Little Ice Age, in *Mechanisms of Global Climate Change at Millennial Time Scales*, *Geophys. Monogr. Ser.*, vol. 112, edited by P. U. Clark, R. S. Webb, and L. D. Keigwin, pp. 35–58, AGU, Washington, D. C.

Bowen, D. Q. (2009), Sea level 400 000 years ago (MIS 11): Analogue for present and future sea-level, *Clim. Past Discuss.*, *5*, 1853–1882, doi:10.5194/cpd-5-1853-2009.

Broecker, W. S. (1994), Massive iceberg discharges as triggers for global climate change, *Nature*, *372*, 421–424, doi:10.1038/372421a0.

Cacho, I., J. O. Grimalt, C. Pelejero, M. Canals, F. J. Sierro, J. A. Flores, and N. Shackleton (1999), Dansgaard-Oeschger and Heinrich event imprints in Alboran Sea paleotemperatures, *Paleoceanography*, *14*(6), 698–705, doi:10.1029/1999PA900044.

Cacho, I., J. O. Grimalt, M. Canals, L. Sbaffi, N. J. Shackleton, J. Schönfeld, and R. Zahn (2001), Variability of the western Mediterranean Sea surface temperature during the last 25,000 years and its connection with the Northern Hemisphere climatic changes, *Paleoceanography*, *16*(1), 40–52, doi:10.1029/2000PA000502.

Chapman, M. R., N. J. Shackleton, and J.-C. Duplessy (2000), Sea surface temperature variability during the last glacial–interglacial cycle: Assessing the magnitude and pattern of climate change in the North Atlantic, *Palaeogeogr. Palaeoclimatol. Palaeoecol.*, *157*(1–2), 1–25, doi:10.1016/S0031-0182(99)00168-6.

Chen, M.-T., Y.-P. Chang, C.-C. Chang, L.-W. Wang, C.-H. Wang, and E.-F. Yu (2002), Late Quaternary sea-surface temperature variations in the southeast Atlantic: A planktic foraminifer faunal record of the past 600 000 yr (IMAGES II MD962085), *Mar. Geol.*, *180*(1–4), 163–181, doi:10.1016/S0025-3227(01)00212-2.

Cortijo, E., L. Labeyrie, L. Vidal, M. Vautravers, M. Chapman, J. C. Duplessy, M. Elliot, M. Arnold, J. L. Turon, and G. Auffret (1997), Changes in sea surface hydrology associated with Heinrich event 4 in the North Atlantic Ocean between 40°N and 60°N, *Earth Planet. Sci. Lett.*, *146*(1–2), 29–45, doi:10.1016/S0012-821X(96)00217-8.

de Abreu, L., N. J. Shackleton, J. Schonfeld, M. Hall, and M. Chapman (2003), Millennial-scale oceanic climate variability off the western Iberian Margin during the last two glacial periods, *Mar. Geol.*, *196*(1–2), 1–20, doi:10.1016/S0025-3227(03)00046-X.

de Abreu, L., F. F. Abrantes, N. J. Shackleton, P. C. Tzedakis, J. F. McManus, D. W. Oppo, and M. A. Hall (2005), Ocean climate variability in the eastern North Atlantic during interglacial marine isotope stage 11: A partial analogue to the Holocene?, *Paleoceanography*, *20*, PA3009, doi:10.1029/2004PA001091.

Desprat, S., M. F. Sánchez Goñi, J. L. Turon, J. F. McManus, M. F. Loutre, J. Duprat, B. Malaizé, O. Peyron, and J.-P. Peypouquet (2005), Is vegetation responsible for glacial inception during periods of muted insolation changes?, *Quat. Sci. Rev.*, *24*(12–13), 1361–1374, doi:10.1016/j.quascirev.2005.01.005.

Desprat, S., M. F. Sánchez Goñi, F. Naughton, J.-L. Turon, J. Duprat, B. Malaizé, E. Cortijo, and J.-P. Peypouquet (2007), Climate variability of the last five isotopic interglacials: Direct land-sea-ice correlation from the multiproxy analysis of north-western Iberian Margin deep-sea cores, in *The Climate of Past Interglacials*, edited by F. Sirocko et al., pp. 375–386, Elsevier, Amsterdam.

de Vernal, A., and C. Hillaire-Marcel (2008), Natural variability of Greenland climate, vegetation, and ice volume during the past million years, *Science*, *320*(5883), 1622–1625, doi:10.1126/science.1153929.

Droxler, A. W., and J. W. Farrell (2000), Marine isotope stage 11 (MIS 11): New insights for a warm future, *Global Planet. Change*, *24*(1), 1–5, doi:10.1016/S0921-8181(99)00065-X.

Eglinton, G., S. Bradshaw, A. Resell, M. Sarnthein, U. Pflaumann, and R. Tiedemann (1992), Molecular record of secular sea surface temperature changes on 100-year timescales for glacial terminations I, II and IV, *Nature*, *356*, 423–426, doi:10.1038/356423a0.

EPICA Community Members (2004), Eight glacial cycles from an Antarctic ice core, *Nature*, *429*, 623–628, doi:10.1038/nature02599.

Eynaud, F., et al. (2009), Position of the Polar Front along the western Iberian Margin during key cold episodes of the last 45 ka, *Geochem. Geophys. Geosyst.*, *10*, Q07U05, doi:10.1029/2009GC002398.

Fiúza, A. F. G. (1983), Upwelling patterns off Portugal, in *Coastal Upwelling, Its Sediment Record*, edited by E. Suess and J. Thiede, pp. 85–98, Plenum, New York.

Fiúza, A. F. G., M. E. Macedo, and M. R. Guerreiro (1982), Climatological space and time variation of the Portuguese coastal upwelling, *Oceanol. Acta*, *5*(1), 31–40.

Flores, J. A., M. Marino, F. J. Sierro, D. A. Hodell, and C. D. Charles (2003), Calcareous plankton dissolution pattern and coccolithophore assemblages during the last 600 kyr at ODP Site 1089 (Cape Basin, South Atlantic): Paleoceanographic implications, *Palaeogeogr. Palaeoclimatol. Palaeoecol.*, *196*(3–4), 409–426, doi:10.1016/S0031-0182(03)00467-X.

Flower, B. P., D. W. Oppo, J. F. McManus, K. A. Venz, D. A. Hodell, and J. L. Cullen (2000), North Atlantic intermediate to deep water circulation and chemical stratification during the past 1 Myr, *Paleoceanography*, *15*(4), 388–403, doi:10.1029/1999PA000430.

Grimalt, J. O., E. Calvo, and C. Pelejero (2001), Sea surface paleotemperature errors in $U_{37}^{K'}$ estimation due to alkenone measurements near the limit of detection, *Paleoceanography*, *16*(2), 226–232, doi:10.1029/1999PA000440.

Guo, Z. T., A. Berger, Q. Z. Yin, and L. Qin (2009), Strong asymmetry of hemispheric climates during MIS-13 inferred from correlating China loess and Antarctica ice records, *Clim. Past*, *5*, 21–31, doi:10.5194/cp-5-21-2009.

Helmke, J. P., H. A. Bauch, U. Röhl, and E. S. Kandiano (2008), Uniform climate development between the subtropical and subpolar northeast Atlantic across marine isotope stage 11, *Clim. Past*, *4*, 181–190, doi:10.5194/cp-4-181-2008.

Hemming, S. R. (2004), Heinrich events: Massive late Pleistocene detritus layers of the North Atlantic and their global climate imprint, *Rev. Geophys.*, *42*, RG1005, doi:10.1029/2003RG000128.

Hodell, D. A., K. A. Venz, C. D. Charles, and U. S. Ninnemann (2003), Pleistocene vertical carbon isotope and carbonate gradients in the South Atlantic sector of the Southern Ocean, *Geochem. Geophys. Geosyst.*, *4*(1), 1004, doi:10.1029/2002GC000367.

Hodell, D. A., J. E. T. Channell, J. H. Curtis, O. E. Romero, and U. Röhl (2008), Onset of "Hudson Strait" Heinrich events in the eastern North Atlantic at the end of the middle Pleistocene transition (~640 ka)?, *Paleoceanography*, *23*, PA4218, doi:10.1029/2008PA001591.

Imbrie, J., et al. (1993), On the structure and origin of major glaciation cycles: 2. The 100,000-year cycle, *Paleoceanography*, *8*(6), 699–735, doi:10.1029/93PA02751.

Jouzel, J., et al. (2007), Orbital and millennial Antarctic climate variability over the past 800,000 years, *Science*, *317*(5839), 793–796, doi:10.1126/science.1141038.

Lebreiro, S. M., J. C. Moreno, I. N. McCave, and P. P. E. Weaver (1996), Evidence for Heinrich layers off Portugal (Tore Seamount: 39°N, 12°W), *Mar. Geol.*, *131*(1–2), 47–56, doi:10.1016/0025-3227(95)00142-5.

Lisiecki, L. E., and M. E. Raymo (2005), A Pliocene-Pleistocene stack of 57 globally distributed benthic $\delta^{18}O$ records, *Paleoceanography*, *20*, PA1003, doi:10.1029/2004PA001071.

López-Martínez, C., J. O. Grimalt, B. Hoogakker, J. Gruetzner, M. J. Vautravers, and I. N. McCave (2006), Abrupt wind regime changes in the North Atlantic Ocean during the past 30,000–60,000 years, *Paleoceanography*, *21*, PA4215, doi:10.1029/2006PA001275.

Loulergue, L., A. Schilt, R. Spahni, V. Masson-Delmotte, T. Blunier, B. Lemieux, J.-M. Barnola, D. Raynaud, T. F. Stocker, and J. Chappellaz (2008), Orbital and millennial-scale features of atmospheric CH_4 over the past 800,000 years, *Nature*, *453*, 383–386, doi:10.1038/nature06950.

Loutre, M. F. (2003), Clues from MIS 11 to predict the future climate – A modelling point of view, *Earth Planet. Sci. Lett.*, *212*(1–2), 213–224, doi:10.1016/S0012-821X(03)00235-8.

Loutre, M. F., and A. Berger (2003), Marine isotope stage 11 as an analogue for the present interglacial, *Global Planet. Change*, *36*(3), 209–217, doi:10.1016/S0921-8181(02)00186-8.

Lüthi, D., et al. (2008), High-resolution carbon dioxide concentration record 650,000–800,000 years before present, *Nature*, *453*, 379–382, doi:10.1038/nature06949.

Martrat, B., J. O. Grimalt, C. Lopez-Martinez, I. Cacho, F. J. Sierro, J. A. Flores, R. Zahn, M. Canals, J. H. Curtis, and D. A. Hodell (2004), Abrupt temperature changes in the western Mediterranean over the past 250,000 years, *Science*, *306*(5702), 1762–1765, doi:10.1126/science.1101706.

Martrat, B., J. O. Grimalt, N. J. Shackleton, L. de Abreu, M. A. Hutterli, and T. F. Stocker (2007), Four climate cycles of recurring deep and surface water destabilizations on the Iberian Margin, *Science*, *317*(5837), 502–507, doi:10.1126/science.1139994.

Maslin, M. A., X. S. Li, M.-F. Loutre, and A. Berger (1998), The contribution of orbital forcing to the progressive intensification of Northern Hemisphere glaciation, *Quat. Sci. Rev.*, *17*(4–5), 411–426, doi:10.1016/S0277-3791(97)00047-4.

Masson-Delmotte, V., et al. (2006), Past temperature reconstructions from deep ice cores: Relevance for future climate change, *Clim. Past*, *2*, 145–165, doi:10.5194/cp-2-145-2006.

McClymont, E. L., A. Rosell-Melé, J. Giraudeau, C. Pierre, and J. M. Lloyd (2005), Alkenone and coccolith records of the mid-Pleistocene in the south-east Atlantic: Implications for the $U_{37}^{K'}$ index and South African climate, *Quat. Sci. Rev.*, *24*(14–15), 1559–1572, doi:10.1016/j.quascirev.2004.06.024.

McManus, J. F., D. W. Oppo, and J. L. Cullen (1999), A 0.5-million-year record of millennial-scale climate variability in the North Atlantic, *Science*, *283*(5404), 971–975, doi:10.1126/science.283.5404.971.

McManus, J., D. Oppo, J. Cullen, and S. Healey (2003), Marine isotope stage 11 (MIS 11): Analog for Holocene and future climate?, in *Earth's Climate and Orbital Eccentricity: The Marine Isotope Stage 11 Question*, *Geophys. Monogr. Ser.*, vol. 137, edited by A. W. Droxler, R. Z. Poore, and L. H. Burckle, pp. 69–85, AGU, Washington, D. C.

Mix, A. C., N. G. Pisias, W. Rugh, J. Wilson, A. Morey, and T. K. Hagelberg (1995), Benthic foraminifer stable isotope record from Site 849 (0–5 Ma): Local and global climate changes, *Proc. Ocean Drill. Program Sci. Results*, *138*, 371–412, doi:10.2973/odp.proc.sr.138.120.1995.

Müller, P. J., G. Kirst, G. Ruhland, I. von Storch, and A. Rosell-Melé (1998), Calibration of the alkenone paleotemperature index $U_{37}^{K'}$ based on core-tops from the eastern South Atlantic and the global ocean (60°N-60°S), *Geochim. Cosmochim. Acta*, *62*(10), 1757–1772, doi:10.1016/S0016-7037(98)00097-0.

Naughton, F., et al. (2009), Wet to dry climatic trend in north-western Iberia within Heinrich events, *Earth Planet. Sci. Lett.*, *284*(3–4), 329–342, doi:10.1016/j.epsl.2009.05.001.

Nave, S., L. Labeyrie, J. Gherardi, N. Caillon, E. Cortijo, C. Kissel, and F. Abrantes (2007), Primary productivity response to Heinrich events in the North Atlantic Ocean and Norwegian Sea, *Paleoceanography*, *22*, PA3216, doi:10.1029/2006PA001335.

Oppo, D. W., J. F. McManus, and J. L. Cullen (1998), Abrupt climate events 500,000 to 340,000 years ago: Evidence from subpolar North Atlantic sediments, *Science*, *279*(5355), 1335–1338, doi:10.1126/science.279.5355.1335.

Pailler, D., and E. Bard (2002), High frequency paleoceanographic changes during the past 140 000 yr recorded by the organic matter in sediments of the Iberian Margin, *Palaeogeogr. Palaeoclimatol. Palaeoecol.*, *181*(4), 431–452, doi:10.1016/S0031-0182(01)00444-8.

Peliz, Á., J. Dubert, A. M. P. Santos, P. B. Oliveira, and B. Le Cann (2005), Winter upper ocean circulation in the western Iberian Basin—Fronts, eddies and poleward flows: An overview, *Deep Sea Res., Part I*, *52*(4), 621–646, doi:10.1016/j.dsr.2004.11.005.

Raffi, I., J. Backman, E. Fornaciari, H. Pälike, D. Rio, L. Lourens, and F. Hilgen (2006), A review of calcareous nannofossil astrobiochronology encompassing the past 25 million years, *Quat. Sci. Rev.*, *25*(23–24), 3113–3137, doi:10.1016/j.quascirev.2006.07.007.

Rodrigues, T., J. O. Grimalt, F. Abrantes, F. Naughton, and J.-A. Flores (2010), The last glacial-interglacial transition (LGIT) in the western mid-latitudes of the North Atlantic: Abrupt sea surface temperature change and sea level implications, *Quat. Sci. Rev.*, *29*(15–16), 1853–1862, doi:10.1016/j.quascirev.2010.04.004.

Rosell-Melé, A., M. Weinelt, M. Sarnthein, N. Koç, and E. Jansen (1998), Variability of the Arctic front during the last climatic cycle: Application of a novel molecular proxy, *Terra Nova*, *10*(2), 86–89, doi:10.1046/j.1365-3121.1998.00172.x.

Roucoux, K. H., P. C. Tzedakis, L. de Abreu, and N. J. Shackleton (2006), Climate and vegetation changes 180,000 to 345,000 years ago recorded in a deep-sea core off Portugal, *Earth Planet. Sci. Lett.*, *249*(3–4), 307–325, doi:10.1016/j.epsl.2006.07.005.

Salgueiro, E., A. H. L. Voelker, L. de Abreu, F. Abrantes, H. Meggers, and G. Wefer (2010), Temperature and productivity changes off the western Iberian Margin during the last 150 ky, *Quat. Sci. Rev.*, *29*(5–6), 680–695, doi:10.1016/j.quascirev.2009.11.013.

Sánchez Goñi, M. F., I. Cacho, J.-L. Turon, J. Guiot, F. J. Sierro, J.-P. Peypouquet, J. O. Grimalt, and N. J. Shackleton (2002), Synchroneity between marine and terrestrial responses to millennial scale climatic variability during the last glacial period in the Mediterranean region, *Clim. Dyn.*, *19*(1), 95–105, doi:10.1007/s00382-001-0212-x.

Shackleton, N. J. (1967), Oxygen isotope analysis and Pleistocene temperature reassessed, *Nature*, *215*, 15–17, doi:10.1038/215015a0.

Shackleton, N. J., A. Berger, and W. R. Peltier (1990), An alternative astronomical calibration

of the lower Pleistocene time scale based on ODP Site 677, *Trans. R. Soc. Edinburgh Earth Sci.*, *81*, 251–261.

Shackleton, N. J., M. A. Hall, and E. Vincent (2000), Phase relationships between millennial-scale events 64,000–24,000 years ago, *Paleoceanography*, *15*(6), 565–569, doi:10.1029/2000PA000513.

Siegenthaler, U., et al. (2005), Stable carbon cycle-climate relationship during the late Pleistocene, *Science*, *310*(5752), 1313–1317, doi:10.1126/science.1120130.

Stein, R., J. Hefter, J. Grützner, A. Voelker, and B. D. A. Naafs (2009), Variability of surface water characteristics and Heinrich-like events in the Pleistocene midlatitude North Atlantic Ocean: Biomarker and XRD records from IODP Site U1313 (MIS 16–9), *Paleoceanography*, *24*, PA2203, doi:10.1029/2008PA001639.

Tzedakis, P. C. (2009), The MIS 11 – MIS 1 analogy, southern European vegetation, atmospheric methane and the "early anthropogenic hypothesis," *Clim. Past Discuss.*, *5*, 1337–1365, doi:10.5194/cpd-5-1337-2009.

Tzedakis, P. C., J. F. McManus, H. Hooghiemstra, D. W. Oppo, and T. A. Wijmstra (2003), Comparison of changes in vegetation in northeast Greece with records of climate variability on orbital and suborbital frequencies over the last 450,000 years, *Earth Planet. Sci. Lett.*, *212*(1–2), 197–212, doi:10.1016/S0012-821X(03)00233-4.

Villanueva, J., J. O. Grimalt, E. Cortijo, L. Vidal, and L. Labeyrie (1997a), A biomarker approach to the organic matter deposited in the North Atlantic during the last climatic cycle, *Geochim. Cosmochim. Acta*, *61*(21), 4633–4646, doi:10.1016/S0016-7037(97)83123-7.

Villanueva, J., C. Pelejero, and J. O. Grimalt (1997b), Clean-up procedures for the unbiased estimation of C_{37} alkenone sea surface temperatures and terrigenous *n*-alkane inputs in paleoceanography, *J. Chromatogr. A*, *757*(1–2), 145–151, doi:10.1016/S0021-9673(96)00669-3.

Voelker, A. H. L., S. M. Lebreiro, J. Schonfeld, I. Cacho, H. Erlenkeuser, and F. Abrantes (2006), Mediterranean outflow strengthening during Northern Hemisphere coolings: A salt source for the glacial Atlantic?, *Earth Planet. Sci. Lett.*, *245*(1–2), 39–55, doi:10.1016/j.epsl.2006.03.014.

Voelker, A., P. Martin, S. M. Lebreiro, and F. Abrantes (2007), Millennial-scale deep/intermediate water changes at the mid-depth Portuguese Margin during marine isotope stage (MIS) 11 (Abstract 0983), *Quat. Int.*, *167–168* (Suppl. 1), 436.

Voelker, A. H. L., T. Rodrigues, R. Stein, J. Hefter, K. Billups, D. Oppo, J. McManus, and J. O. Grimalt (2009), Variations in mid-latitude North Atlantic surface water properties during the mid-Brunhes: Does marine isotope stage 11 stand out?, *Clim. Past Discuss.*, *5*, 1553–1607, doi:10.5194/cpd-5-1553-2009.

Wright, A. K., and B. P. Flower (2002), Surface and deep ocean circulation in the subpolar North Atlantic during the mid-Pleistocene revolution, *Paleoceanography*, *17*(4), 1068, doi:10.1029/2002PA000782.

Yin, Q. Z., and Z. T. Guo (2007), Strong summer monsoon during the cool MIS-13, *Clim. Past Discuss.*, *3*, 1119–1132, doi:10.5194/cpd-3-1119-2007.

Zachos, J., M. Pagani, L. Sloan, E. Thomas, and K. Billups (2001), Trends, rhythms, and aberrations in global climate 65 Ma to present, *Science*, *292*(5517), 686–693, doi:10.1126/science.1059412.

Zahn, R., J. Schönfeld, H.-R. Kudrass, M.-H. Park, H. Erlenkeuser, and P. Grootes (1997), Thermohaline instability in the North Atlantic during meltwater events: Stable isotope and ice-rafted detritus records from Core SO75-26KL, Portuguese Margin, *Paleoceanography*, *12*(5), 696–710, doi:10.1029/97PA00581.

F. Abrantes, F. Naughton, T. Rodrigues, and A. H. L. Voelker, Unidade Geologia Marinha, LNEG, P-2721-866 Lisboa, Portugal. (teresa.rodrigues@ineti.pt)

J. O. Grimalt, Department of Environmental Chemistry, Institute of Environmental Assessment and Water Research, E-08034 Barcelona, Spain.